Renewable Energy 162 (2020) 249–256

Contents lists available at ScienceDirect

Renewable Energy

journal homepage: www.elsevier.com/locate/renene

Failure signature classification in solar photovoltaic plants using RGB images and convolutional neural networks

Alejandro Rico Espinosa *, Michael Bressan , Luis Felipe Giraldo

Universidad de Los Andes, Bogota, Colombia

ARTICLE INFO

Article history:
Received 13 May 2020
Received in revised form
29 July 2020
Accepted 31 July 2020
Available online 10 August 2020

Keywords:
Photovoltaic system
RGB images
Semantic segmentation
Convolutional neural network

ABSTRACT

Physical fault detection in panels that are part of photovoltaic (PV) plants typically involves the analysis of thermal and electroluminescent images, which makes it either difficult or impossible to identify the source of the fault in the plant. This paper proposes a method of automatic physical fault classification for PV plants using convolutional neural networks for semantic segmentation and classification from RGB images. This study shows experimental results for 2 output classes identified as a fault and no fault, and 4 output classes as no fault, cracks, shadows, and dust that cannot be easily detected. The proposed method presents an average accuracy of 75% for 2 output classes and 70% for 4 classes, showing a positive approach to the proposed classification method for PV systems.

1. Introduction

Solar photovoltaic (PV) systems increased its installed capacity around the world from 40.277 MW to 580.159 MW in only 9 years (2010–2019) due to the benefits that this type of renewable energy offers. Despite this fact, this technology still needs to be developed because it currently has a very low efficiency (15%–20%). Therefore, it is important to study every source of loss in the system since PV systems are sensitive to fault occurrences [1]. The study in [2] categorizes typical faults that occur in PV power plants in i) panel faults, ii) faults associated with shadow, and iii) electrical faults. To detect the presence of a fault in any of these categories, it is usual to study the current-voltage (I-V) characteristic curve since anomalies in the generation process modify its shape [3,4]. However, identifying the cause of the fault is still a challenging task since many of these models in literature do not consider the effect of reverse bias. Deeper analysis of I-V curves is required to identify faults [3,5]. Also, regular manual checks are time-consuming, costly, and laborious in large scales systems [6]. In any case, identifying the cause of a fault in a solar panel facilitates defining and taking actions to mitigate impacts on the efficiency of the PV system. In this paper, we propose a methodology to do this based on RGB images as the source of information.

Some of the fault signature sources that are most challenging to identify are the causes of partial shading in solar panels. Because of current mismatch due to the presence of partial shading, the efficiency of the PV modules decreases drastically and increases the risk of hot spots [4]. A hot spot refers to a temperature increase due to power dissipation in a reverse-biased cell [7]. Several solutions based on the implementation of electrical devices and simulation tools have been recently proposed to mitigate the impact of shading in PV systems [5,8–10]. However, most of these approaches can be difficult and expensive to implement, and they do not allow the accurate detection of physical scenarios that generate hot spots in a solar array. It is important to minimize the use of additional electrical devices to avoid increasing costs and the complexity of the system.

Recent alternative methodologies for detecting problems caused by partial shading in solar panels involve pattern recognition on images. For example, a canny filter has been used to highlight imperfections in solar panels to facilitate the detection conducted by a human expert [11,12]. Another technique uses electroluminescent imaging for the detection of surface imperfections, typically implemented during panel manufacturing. The work in [13] proposes an automatic surface defect detector for PV cells using electroluminescent images. They compared the use of a convolutional neural network (CNN) and a support vector machine (SVM) to conduct a binary classification (damage or not),

* Corresponding author. University of the Andes, Cra 1 Nº 18A-12, Bogota, Colombia.
E-mail addresses: aa.rico@uniandes.edu.co (A. Rico Espinosa), m.bressan@uniandes.edu.co (M. Bressan), lf.giraldo404@uniandes.edu.co (L.F. Giraldo).

https://doi.org/10.1016/j.renene.2020.07.154
0960-1481/

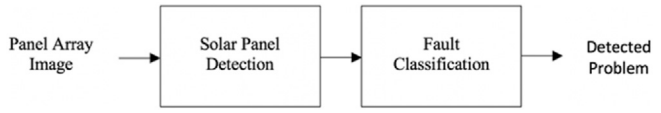

Fig. 1. A proposed methodology for fault detection and classification.

concluding that than a CNNs can potentially outperform SVMs for image classification. Also, thermal imaging has used for problem identification in solar farms. The work of [14] uses CNNs to identify heating points in solar arrays based on thermal images.

Most of the studies that have been proposed to analyze faults signatures in solar panels allow for the detection of damage but do not classify the source of the problem. In this letter, our contribution is to introduce a methodology to detect, based on RGB images, whether there is a signature of failure or not, and the type of sources that can generate the hot spots. This methodology aims to provide a support tool for traditional fault recognition techniques through an automatic system for detection and classification, reducing time and effort in large scale PV systems. Using segmentation and classification techniques based on deep learning on RGB images, our method (Section 2) conducts a fast potential problems detection and classification (Section 3), reducing audit efforts and implementation costs. We aim to classify between 4 classes of factors that can lead to a power reduction (Section 4) and are typically difficult to be automatically detected in PV arrays: shadows, breakages, visible dust, and no fault. Distinguishing between shadows and dust is important since opacity levels might differ. While partial shading reduces solar irradiance, dust creates a tiny layer of particles that covers the PV surface affecting the overall energy delivery [1]. The learning process was conducted on an image database that we collected and manually labeled. We see this work as an important step in the formulation of methodologies that integrate different sources of information and pattern recognition technologies in solar photovoltaic systems.

2. Methodology

The proposed methodology has two main blocks, as it is illustrated in Fig. 1. Given an RBG image of a solar panel array under an unknown perspective, the first step is to extract the panel objects using a CNN, removing environmental noise. In this step, we apply the process known as semantic segmentation [15,16]. Then, fault detection and classification is done using CNN as well [17,18]. Following, we explain how we constructed the training databases and implementation details of the networks for segmentation and classification.

2.1. Construction of the database

Multiple databases were used during the entire process. Most of the images were taken from different internet search engines that provide images of solar installations around the world. A smaller portion of the images was taken from local installations, such as the international airport and panels at the university campus. In this study, we considered RBG images that i) have a perspective where the panel surface is clearly shown, and ii) whose quality is such that a human eye can identify failures. We took 345 images of size 200×200, where each was manually pixel labeled with label 0 for background and 1 for the photovoltaic panel. For the solar panel detection stage, a CNN was trained for semantic segmentation using a subset of 145 images. The remaining 200 images were used for the classification study. In this dataset, images belonged to fault classes 'cracks', 'shadow', 'dust', and 'no-fault', 50 images per class. Although the testing dataset is larger than the training one for the segmentation stage, results show a low error in pixel classification, showing that the number of training images was sufficient to conduct image segmentation during the classification stage.

2.2. The architecture of the convolutional neural network

We use CNNs to do solar panel detection and classification tasks. Fig. 2 shows the usual architecture for this type of network. Typically, a CNN has two main stages: a stage where convolution and down-sampling processes (max pooling) are conducted, and a stage with a fully connected neural network. The first stage identifies those filters that are needed to extract the most important features of the images at different levels of granularity [19]. At the second stage, the fully connected layer is set to share information between a huge number of neurons that search relations and patterns to assign a probability for each of the defined outputs (classes) depending on their labels. Due to its topology and the way it transforms input information, CNNs are highly used for image classification problems [19].

The architecture of the CNN used for semantic segmentation uses 4 convolutional layers. Each is followed by a set of ReLu units (to set negative values to zero) and max pooling layers. After the last convolution, a fully connected and a layer with SoftMax activation functions were used. Convolutional layers for this topology use 3×3 filters. The architecture of the CNN used for fault classification was more complex than the one used for semantic segmentation. It is composed of 5 convolutional layers use 5×5 filters. Each convolutional layer was followed by a batch normalization Layer (to speed up the process), a layer with ReLu units, and a max pooling layer. Similar to what was implemented in the semantic

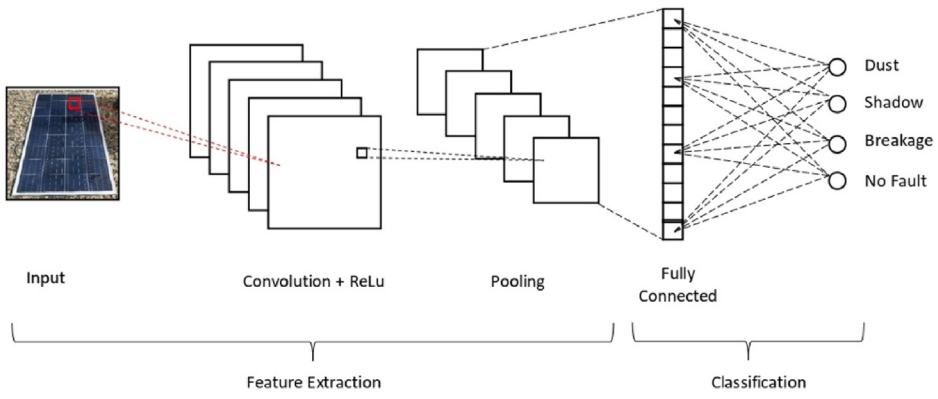

Fig. 2. CNN topology.

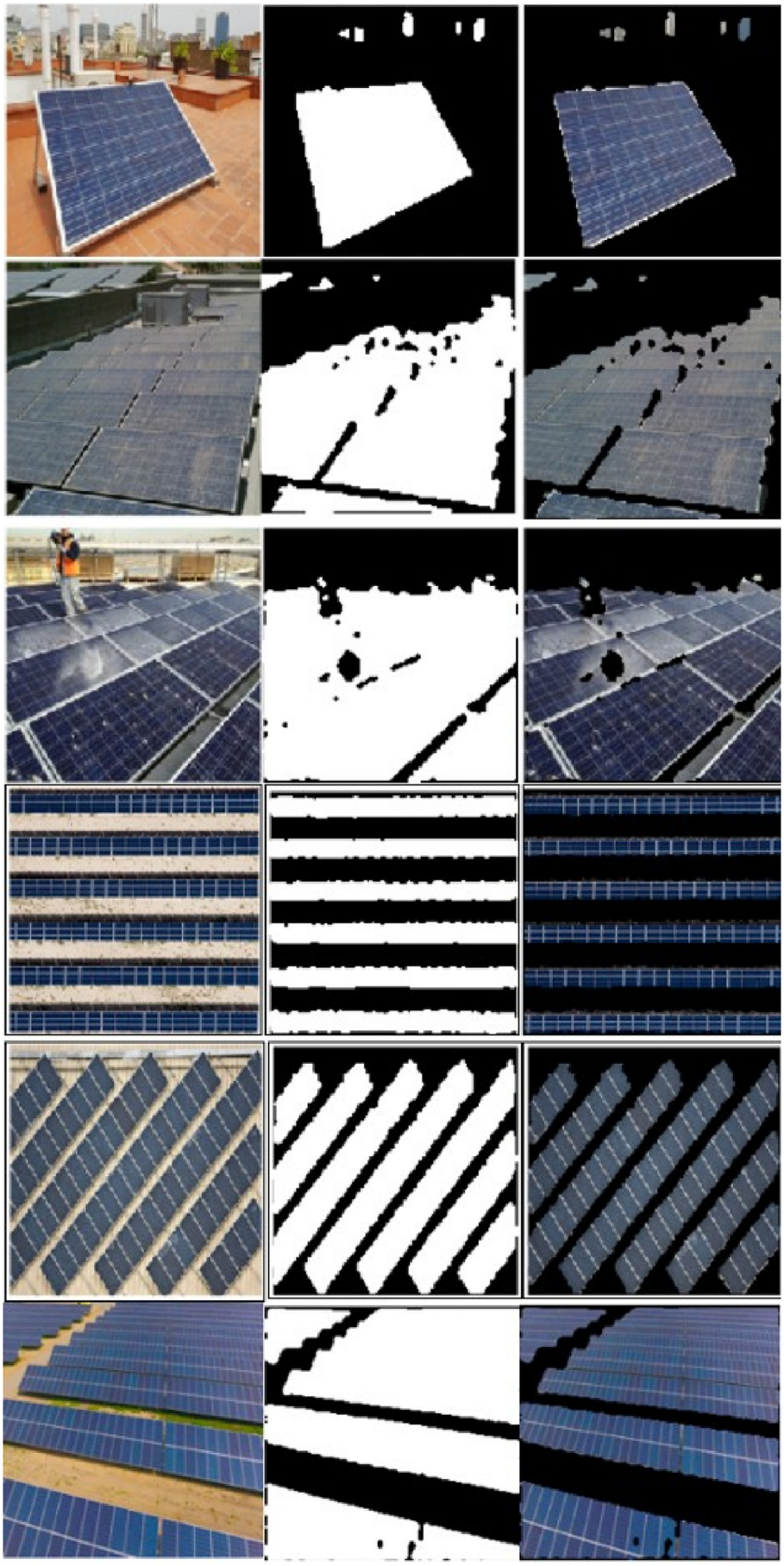

Fig. 3. Examples of solar panel segmentation using a CNN for semantic segmentation.

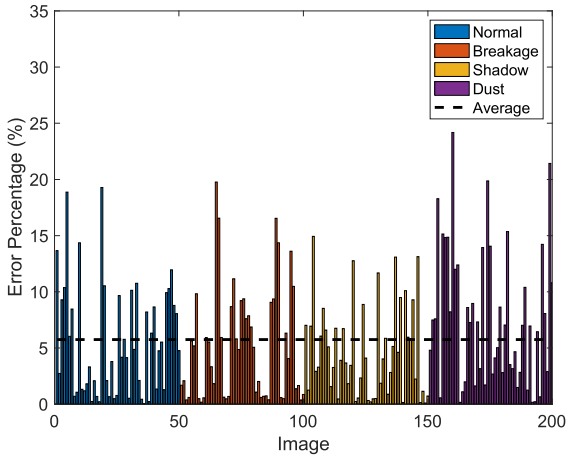

Fig. 4. Percentage error of pixel classification for each test image in the segmentation stage of the proposed methodology.

Fig. 5. One of the learned filters on CNN for panel segmentation.

segmentation network, a fully connected layer with SoftMax activations were used to do classification. These parameters are typical when using CNN for classification tasks in images [11–14]. We implemented the learning process using the deep learning toolbox in MATLAB.

3. Solar panel detection results

The semantic segmentation method uses one label per each pixel on the image. This method allows us to distinguish between background and solar panels, creating a mask for the solar panels. We used 145 images that were manually labeled for training, and 200 for testing. These testing images are the ones that are used for classification. Some results of the solar panel detection using this method are shown in Fig. 3. Note that faulty panels (including dust, breakages, and shadows) at different perspectives can be segmented with this method. Fig. 4 shows the percentage of pixel segmentation error for each one of the 200 tested images. From this set of results, note that the average segmentation error is 5.75%, where the worst segmentation error is 24%. It is important to mention that we tested the YOLO (You Only Look Once) algorithm to identify solar panels [20], but the semantic segmentation approach provided more precise segmentation results. YOLO is an object detection algorithm based on a slide window approach to recognize specific objects in real-time. Here, a set of anchor boxes is pre-defined in which their size is determinated by clustering typical values of the object to be recognized.

One of the filters at a convolutional layer that was learned is shown in Fig. 5, and some of the images that resulted from applying this filter for solar panel segmentation are shown in Fig. 6. Note that this filter, as many of the learned filters at the convolutional layers, tends to highlight the edges in the image. This is an expected result given the geometry of the panels, allowing the fully connected layer of the network to accurately classify between panel and background regions.

4. Fault classification results

Once the solar panel is properly segmented in the image, we proceed to classify the solar panel according to the physical fault signatures. The selected classes are: 'breakage', 'shadow', 'dust', 'no-fault'. A set of 200 images containing images for each one of the classes was manually labeled to evaluate the performance of the classification system. Besides computing the classification accuracy, we calculate recall, precision, and *F1* scores to have a complete assessment of the classification model [21]. Let TP_i be the number of correctly predicted images from class i (true positives), TN_i be the number of correctly predicted images that are not from class i (true negative), FP_i be the number of images incorrectly predicted as class i (false positives), and FN_i be the number of images from class i that are incorrectly classified (false negatives). Recall γ_i and precision ρ_i for class i are computed as

$$\gamma = \frac{TP_i}{TP_i + FN_i}\ ,\ \rho = \frac{TP_i}{TP_i + FP_i} \tag{1}$$

F1 index is the weighted average of recall and precision in Equation (1) and is computed as

$$F1 = 2\frac{\gamma\rho}{\gamma + \rho} \tag{2}$$

Following, we show the results of the classification stage of the proposed methodology. We first explore the case when we have a binary classification ('fault', 'no-fault'), to later study the four-class classification case.

4.1. Classification for 2 output classes

To evaluate the ability of the model to conduct binary classification, first, we took the 50 images of class 'no-fault'. To create the class 'fault', 17 images were randomly selected from each of the remaining datasets in the study (breakages, shadow, dust) to complete a total of 51 images for this class. Then, we estimated the classification accuracy, recall, precision, and *F1* scores using a 4-fold crossvalidation, and repeated the process 10 times. Fig. 7 shows the average accuracy and loss during training (solid line) and testing (dashed line) along time for one of the batches. Note that, during the training process, the model can learn a pattern despite the small size of the dataset.

Tables 1 and 2 show the confusion matrix and the computation of average recall, precision, and F1 scores from Equations (1) and (2). In this case, detecting faults of the PV system with RGB images reaches an average accuracy of 75.39%, showing the ability of the model to detect whether there is a fault in the solar panel or not. Also, Table 2 shows the computation of average recall, precision, and F1 scores. Note that these are reasonably good values that are above a 0.7 threshold.

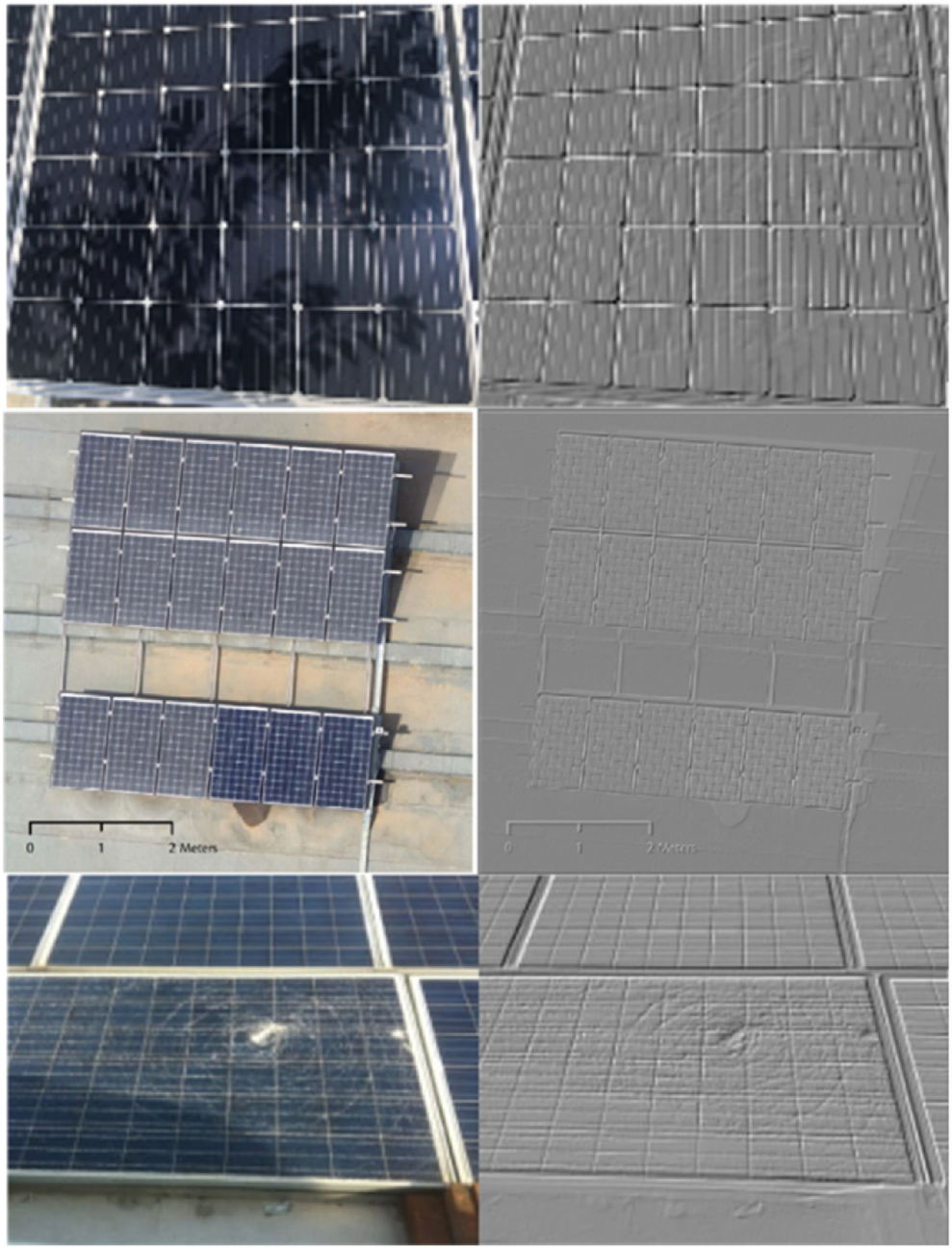

Fig. 6. Images after one of the convolutions in the CNN.

4.2. Classification for 4 output classes

In a similar fashion that it was done in the binary classification case, we evaluate the ability of the model to conduct a 4-class classification task. Remember that the physical fault signature classes are breakages, dust, and shadows. We estimated the classification accuracy, recall, precision, and *F1* scores using a 4-fold crossvalidation scheme. Fig. 8 shows the average accuracy and loss during training (solid line) and testing (dashed line) along time for one of the batches. Note that in this case, during the training process, the model is able to learn a pattern despite the small size of the dataset as well.

We also studied the filtered images at the convolutional layer of CNN for classification. Fig. 9 is the filter with the largest activation at one of the convolutional layers of the model, and Fig. 10 shows images with failures that result from applying the convolution process. As opposed to the segmentation task, CNN for classification uses filters to discard quick changes in contrast, allowing the fully connected network to focus on those patterns that reveal the presence of shadows, visible dust, and cracks that occupy big portions of the panel. Small breakages and cracks can be filtered out from the image in this layer, which explains the low classification rates for this class.

Tables 3 and 4 show the confusion matrix and the computation of average recall, precision, and F1 scores. Note that 'no-fault', 'dust', and 'shadows' classification have the highest accuracy scores

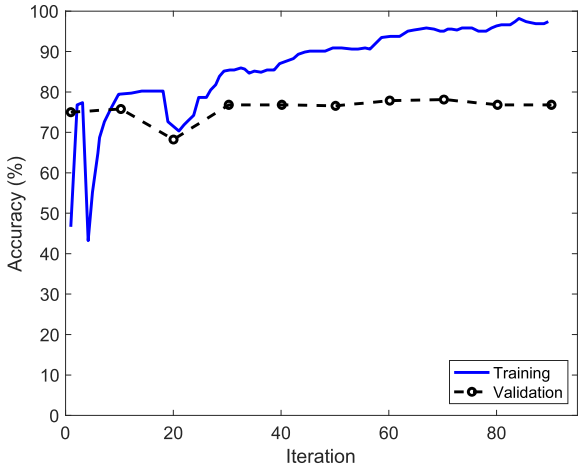

(a)

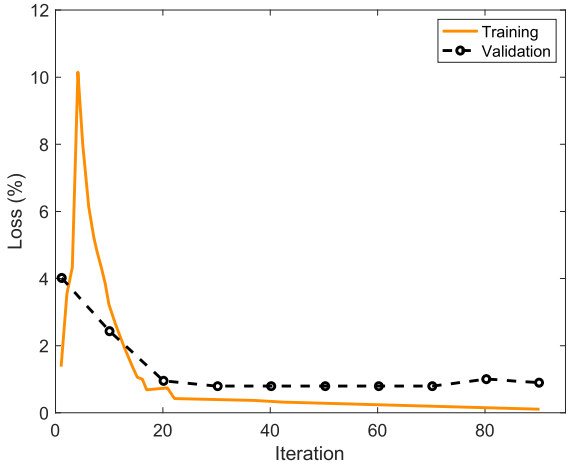

(b)

Fig. 7. (a) Average accuracy and (b) loss along time for one of the batches in the binary classification task. The solid line corresponds to training and the dashed line corresponds to testing.

Table 1
Confusion Matrix for the binary classification task.

	Fault	No Fault
Fault	75.39%	24.61%
No Fault	30.00%	70.00%

Table 2
Average recall, precision, and *F*1 scores for the binary classification task.

Recall	Precision	F1
0.7539	0.7153	0.73

(almost 70%, 65.71%, and 41.03%).

Even though class 'breakage' has an average error above chance, it has a high classification error, showing that it is a difficult task to solve. The model tends to overlook cracks in the images, classifying them as 'no-fault' images. Also, the recall, precision, and F1 scores showed a reasonable classification ability of the CNN. In general,

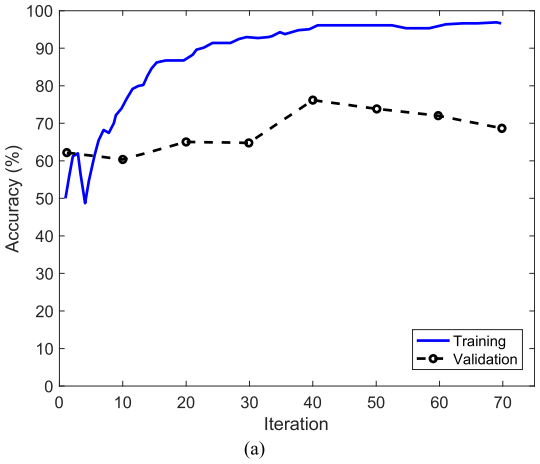

(a)

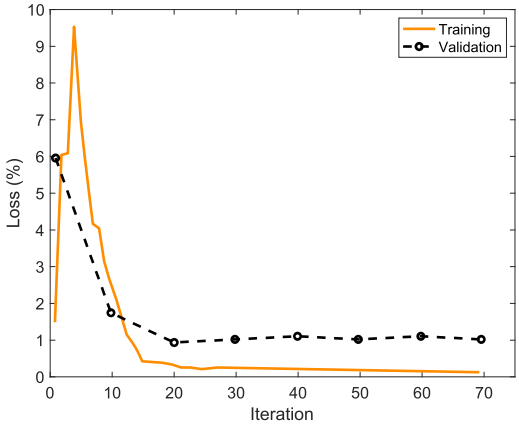

(b)

Fig. 8. (a) Accuracy and (b) loss along time for one of the batches in the four-class classification task. The solid line corresponds to training and the dashed line corresponds to testing.

Fig. 9. Largest activation filter.

these results lead us to argue that the proposed methodology can actually differentiate the types of failures signatures presented in PV systems.

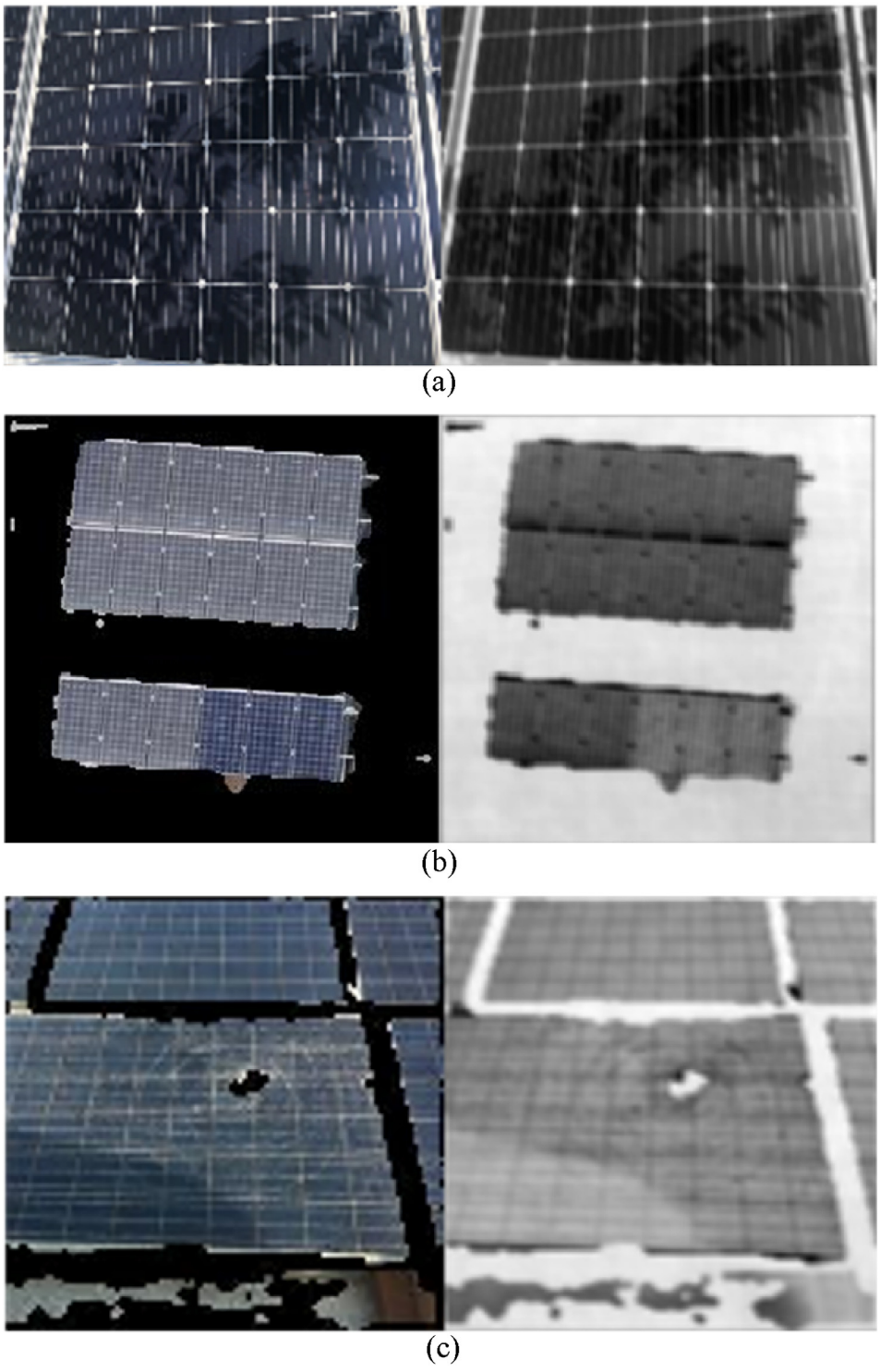

Fig. 10. Output images from a convolutional layer of the learned model for classification for images with (a) shadows, (b) dust, and (c) breakages.

Table 3
Confusion Matrix for the 4-class classification task.

	Breakages	Shadows	Dust	No Fault
Breakages	28.21%	18.43%	22.59%	30.77%
Shadows	24.36%	41.03%	10.42%	24.20%
Dust	12.18%	2.08%	69.23%	16.51%
No Fault	11.86%	14.26%	8.17%	65.71%

Table 4
Average recall, precision, and *F*1 scores for the four-class classification task.

Class	Recall	Precision	*F*1
Breakage	0.2821	0.3682	0.32
Shadow	0.4103	0.5413	0.47
Dust	0.6923	0.6270	0.66
No fault	0.6571	0.4790	0.55

5. Conclusions and future work

A methodology for the automatic physical fault signatures detection and classification in photovoltaic panels from RGB images is presented. This methodology is based on a solar panel detection stage and a factor of decreasing the PV performance classification stage. Detection is conducted by a convolutional neural network for semantic segmentation, and classification is conducted by a convolutional neural network that classifies between breakages, shadows, dust, and no fault. The models were trained using images that were collected and manually labeled. It is shown that the proposed methodology is able to practically detect panels in a given image, and to do binary classification (fault, no-fault) and 4-class classification. Even though the collected dataset is relatively small, an accuracy up to 70% is obtained for the 4-class classification case, showing that the proposed method can be a powerful solution for physical problem detection to be implemented in systems with PV panels.

Future work includes the optimization of the parameters and architectural values used for segmentation and classification. Additionally, this study considered real scenarios that included images from various PV systems in non-controlled conditions (e.g., angles, quality, range). We believe that increasing the image dataset will help to improve the performance of the CNN. Also, the study of more scenarios can be considered, such as the inclusion of other types of issues that can decrease PV performance and the implementation of these models in portable devices for real-time processing.

CRediT authorship contribution statement

Alejandro Rico Espinosa: Conceptualization, Methodology, Software, Investigation, Writing - original draft, Writing - review & editing. **Michael Bressan:** Methodology, Writing - review & editing, Supervision. **Luis Felipe Giraldo:** Methodology, Writing - review & editing, Supervision.

Declaration of competing interest

The authors declare that they have no known competing financial interests or personal relationships that could have appeared to influence the work reported in this paper.

Acknowledgment

We would like to thank the Information and Technology Services Department (DSIT) and the School of Engineering at Universidad de Los Andes, which supplied the storage capacity needed to conduct this research.

References

[1] Mohammad Reza Maghami, Hashim Hizam, Chandima Gomes, Mohd Amran Radzi, Mohammad Ismael Rezadad, Shahrooz Hajighorbani, Power loss due to soiling on solar panel: a review, Renew. Sustain. Energy Rev. 59 (2016) 1307–1316.
[2] D.S. Pillai, N. Rajasekar, A comprehensive review on protection challenges and fault diagnosis in pv systems, Renew. Sustain. Energy Rev. 91 (2018) 18–40.
[3] Y.E. Basri, M. Bressan, L. Seguier, H. Alawadhi, C. Alonso, A proposed graphical electrical signatures supervision method to study pv module failures, Sol. Energy 116 (2015) 247–256.
[4] M. Bressan, Y.E. Basri, A. Galeano, C. Alonso, A shadow fault detection method based on the standard error analysis of i-v curves, Renew. Energy 99 (2016) 1181–1190.
[5] K.A. Kim, P.T. Krein, Reexamination of photovoltaic hot spotting to show inadequacy of the bypass diode, IEEE J. Photovoltaics 5 (2015) 1435–1441.
[6] D. Ji, C. Zhang, M. Lv, Y. Ma, N. Guan, Photovoltaic array faultdetection by automatic reconfiguration, Energies 10 (2017) 699, https://doi.org/10.3390/en10050699.
[7] K.A. Kim, P.T. Krein, Hot spotting and second breakdown effects on reverse i-v characteristics for mono-crystalline si photovoltaics, in: 2013IEEE Energy Conversion Congress and Exposition, 2013, pp. 1007–1014.
[8] S. Daliento, F.D. Napoli, P. Guerriero, V. d'Alessandro, A modified bypass circuit for improved hot spot reliability of solar panels subject to partial shading, Sol. Energy 134 (2016) 211–218.
[9] V. D'Alessandro, F.D. Napoli, P. Guerriero, S. Daliento, An automated high-granularity tool for a fast evaluation of the yield of pv plants accounting for shading effects, Renew. Energy 83 (2015) 294–304.
[10] M. Bressan, A. Gutierrez, L.G. Gutierrez, C. Alonso, Development of a real-time hot-spot prevention using an emulator of partially shaded pv systems, Renew. Energy 127 (2018) 334–343.
[11] S. Vergura, O. Falcone, Filtering and processing ir images of pv mod- ules, Renew. Energy Power Qual. J. 1 (9) (2011) 1209–1214.
[12] J.A. Tsanakas, D. Chrysostomou, P.N. Botsaris, A. Gasteratos, Fault diagnosis of photovoltaic modules through image processing and canny edge detection on field thermographic measurements, Int. J. Sustain. Energy 34 (2015) 351–372.
[13] S. Deitsch, V. Christlein, S. Berger, C. Buerhop-Lutz, A. Maier, F. Gallwitz, C. Riess, Automatic Classification of Defective Photovoltaic Module Cells in Electroluminescence Images, 2018 arXiv preprint arXiv, 1807.02894.
[14] R. Pierdicca, E. Malinverni, F. Piccinini, M. Paolanti, A. Felicetti, P. Zin- garetti, Deep convolutional neural network for automatic detection of damaged photovoltaic cells, Int. Arch. Photogram. Rem. Sens. Spatial Inf. Sci. 42 (2018).
[15] J. Long, E. Shelhamer, T. Darrell, Fully convolutional networks for se- mantic segmentation, in: Proceedings of the IEEE Conference on Computer Vision and Pattern Recognition, 2015, pp. 3431–3440.
[16] Juan Jose Rubio, Takahiro Kashiwa, Teera Laiteerapong, Wenlong Deng, Kohei Nagai, Sergio Escalera, Kotaro Nakayama, Yutaka Matsuo, Helmut Prendinger, Multi-class structural damage segmentation using fully convolutional networks, Comput. Ind. 112 (2019).
[17] G. Yao, T. Lei, J. Zhong, A review of convolutional-neural-network- based action recognition, Pattern Recogn. Lett. 118 (2019) 14–22.
[18] Renxiang Chen, Xin Huang, Lixia Yang, Xiangyang Xu, Xia Zhang, Yong Zhang, Intelligent fault di- agnosis method of planetary gearboxes based on convolution neural net- work and discrete wavelet transform, Comput. Ind. 106 (2019) 48–59.
[19] I. Goodfellow, Y. Bengio, A. Courville, Deep Learning, MIT press, 2016.
[20] J. Redmon, S. Divvala, R. Girshick, A. Farhadi, You only look once: unified, real-time object detection, in: Proceedings of the IEEE Conference on Computer Vision and Pattern Recognition, 2016, pp. 779–788.
[21] P. Flach, M. Kull, Precision-recall-gain curves: Pr analysis done right. Advances in Neural Information Processing Systems, 2015, pp. 838–846.